

Infrared behavior and Gribov ambiguity in $SU(2)$ lattice gauge theory

V. G. Bornyakov

*Institute for High Energy Physics, 142281, Protvino, Russia
and Institute of Theoretical and Experimental Physics, 117259 Moscow, Russia*

V. K. Mitrjushkin

*Joint Institute for Nuclear Research, 141980 Dubna, Russia
and Institute of Theoretical and Experimental Physics, 117259 Moscow, Russia*

M. Müller-Preussker

*Humboldt-Universität zu Berlin, Institut für Physik, Newton-Strasse 15, 12489 Berlin, Germany
(Received 30 January 2009; published 9 April 2009)*

For $SU(2)$ lattice gauge theory, we study numerically the infrared behavior of the Landau-gauge ghost and gluon propagators with a special accent on the Gribov copy dependence. Applying a very efficient gauge-fixing procedure and generating up to 80 gauge copies, we find that the Gribov copy effect for both propagators is essential in the infrared. In particular, our *best copy* dressing function of the ghost propagator approaches a *plateau* in the infrared, while for the random *first copy* it continues to grow. Our *best copy* zero-momentum gluon propagator shows a tendency to *decrease* with growing lattice size, which excludes singular solutions. Our results seem compatible with the so-called *decoupling solution* with a nonsingular gluon propagator. However, we do not yet consider the Gribov copy problem to be resolved.

DOI: 10.1103/PhysRevD.79.074504

PACS numbers: 11.15.Ha, 12.38.Gc, 12.38.Aw

I. INTRODUCTION

The lattice study of the gluon and ghost propagators in Landau gauge has a long history, beginning with the work of Mandula and Ogilvie [1] (for a review see, e.g., [2,3] and references therein). One of the main goals of such studies was to clarify the infrared (IR) asymptotics of the propagators and of the running coupling which can be determined through these propagators. The hope was always that *ab-initio* lattice results would give support to or discriminate between various theoretical predictions for the IR behavior obtained with continuum methods, in particular, within the Dyson-Schwinger (DS) approach. One previous assumption about confinement was definitely overturned: lattice results showed that the gluon propagator has no $1/p^4$ IR singularity.

At the same time, it has been found that the lattice approach has its own difficulties when applied to such studies. One of them is that, to reach the small momenta that are necessary to study the IR limit, one has to use huge lattices, which makes the numerical simulations formidable. Another less apparent, but not less difficult problem is the existence of Gribov copies. Although for many years it was believed that the effect of Gribov copies on both gluon and ghost propagators was weak and could be considered just as a noise in the scaling region [2,4], it has been found, first for the ghost propagator [5] and quite recently for the gluon propagator [6], that these effects are in fact quite strong. The presence of these effects makes the task of lattice computation of the field propagators in the IR region even more difficult.

These difficulties of the lattice approach have made it impossible so far to obtain results which could confirm or disprove the existent confinement scenarios proposed by Gribov [7] and Zwanziger [8] on one hand, and by Kugo and Ojima [9,10] on the other. The Gribov-Zwanziger scenario predicts that the gluon propagator is IR vanishing, while both approaches point to an IR divergent ghost dressing function.

In recent years the interest in the lattice results for field propagators in the IR region has been revived. This interest was also stimulated by the practical progress achieved over the years within the DS approach, as pursued by Alkofer, von Smekal, and others (for an intermediate review see [11]), and more recently with the help of functional renormalization group (FRG) equations [12,13]. Infrared QCD has also been investigated using the stochastic quantization method [14,15], as well as with effective actions [16,17].

In this paper we continue our lattice study of the influence of Gribov copies on the (minimal) Landau-gauge $SU(2)$ gluon and ghost propagators in the IR region by applying global $Z(2)$ flip transformations in combination with an effective optimization algorithm, the so-called *simulated annealing* (SA). The flip transformation was introduced in [6]. Its influence on the gluon propagator was thoroughly studied later [18]. The $Z(2)$ flips—equivalent to nonperiodic $Z(2)$ gauge transformations—were shown to cause rather strong effects in the IR behavior of the gluon propagator. In [18] high statistics computations of the gluon propagator were made for lattice sizes varying from 1.8 fm to 6.5 fm at one fixed bare lattice coupling

$\beta = 4/g_0^2 = 2.20$. The latter was chosen in order to reach reasonably large physical volumes (and thus small momenta) on comparatively moderate lattice sizes up to 32^4 . It turned out that due to better gauge fixing, finite-volume effects, which are usually strong at minimal momenta, became largely suppressed. Furthermore, it has been observed that at momenta $p \sim 270$ MeV the gluon propagator seems to have a turning point, leaving open the possibility for a vanishing gluon propagator in the IR limit $p^2 \rightarrow 0$. Here we continue this investigation, enlarging the lattice up to 40^4 at the same β value corresponding to a volume of $(8.4 \text{ fm})^4$ and extending the studies to the ghost propagator, too. We systematically search for Gribov copies by combining all $2^4 = 16$ $Z(2)$ Polyakov loop sectors for all Euclidean directions into one gauge orbit.

The main motivation for this computation is triggered by the puzzle posed by the above-mentioned continuum approaches. Various kinds of solutions with a quite different IR behavior of the gluon and ghost propagators have been reported by several groups. The powerlike solution with a relation between gluon κ_D and ghost $\kappa_G > 0$ exponents $\kappa_D = -2\kappa_G$ was recently called a *scaling solution* [19]. This solution [13,14,20–23] allows the gluon propagator to vanish and the ghost dressing function to diverge in the IR limit in one-to-one correspondence with both the Gribov-Zwanziger scenario [7,24] and the Kugo-Ojima criterion [9,10] for confinement. On the contrary, the so-called *decoupling solutions* [17,25–27] provide an IR finite or weakly divergent gluon propagator and a finite ghost dressing function, leading to a running coupling vanishing in the infrared. For recent discussions of the present status of research see, e.g., [19] and further references therein.¹ The lattice approach based on the first-principles path integral quantization should be able to resolve the issue.

Results for $SU(2)$ [28] as well as for $SU(3)$ [29] obtained on very large lattices and by employing purely periodic gauge transformations seem to be in conflict with the scaling solution and are compatible with the decoupling solution. It has recently been pointed out in [30] that this might not be in conflict with the (appropriately modified) Gribov-Zwanziger scenario.

Here, by enlarging the gauge orbits with nonperiodic $Z(2)$ flip gauge transformations and employing the SA algorithm, we shall come closer to the global extremum of the Landau-gauge functional, i.e. closer to the fundamental modular region.²

We find the Gribov copy dependence to be very strong. Still, our results look rather like an argument in favor of the decoupling solution with a nonsingular gluon propagator. However, we do not yet consider the problem of Gribov

copies and, correspondingly, the infrared asymptotics of the gluon propagator to be resolved.

In Sec. II we introduce the observables to be computed. In Sec. III some details of the gauge-fixing method and of the simulation are given, whereas in Sec. IV we present our results. Before coming to the conclusions in Sec. VI, we will discuss the dependence of our results on the number of gauge copies in Sec. V.

II. GLUON AND GHOST PROPAGATORS: THE DEFINITIONS

For the Monte Carlo generation of ensembles of non-gauge-fixed gauge field configurations, we use the standard Wilson action, which for the case of an $SU(2)$ gauge group is written

$$S = \beta \sum_x \sum_{\mu > \nu} \left[1 - \frac{1}{2} \text{Tr}(U_{x\mu} U_{x+\mu;\nu} U_{x+\nu;\mu}^\dagger U_{x\nu}^\dagger) \right], \quad (1)$$

$$\beta = 4/g_0^2.$$

Here g_0 is a bare coupling constant and $U_{x\mu} \in SU(2)$ are the link variables. The latter transform under gauge transformations g_x as follows:

$$U_{x\mu} \xrightarrow{g_x} U_{x\mu}^g = g_x^\dagger U_{x\mu} g_{x+\mu}, \quad g_x \in SU(2). \quad (2)$$

The standard definition [1] of the dimensionless lattice gauge vector potential $\mathcal{A}_{x+\hat{\mu}/2,\mu}$ is

$$\mathcal{A}_{x+\hat{\mu}/2,\mu} = \frac{1}{2i} (U_{x\mu} - U_{x\mu}^\dagger) \equiv A_{x+\hat{\mu}/2,\mu}^a \frac{\sigma_a}{2}. \quad (3)$$

The reader should keep in mind that the definition is not unique, which can have an essential influence on the propagator results in the IR region, where the continuum limit is hard to control.

In lattice gauge theory the usual choice for the Landau-gauge condition is [1]

$$(\partial \mathcal{A})_x = \sum_{\mu=1}^4 (\mathcal{A}_{x+\hat{\mu}/2,\mu} - \mathcal{A}_{x-\hat{\mu}/2,\mu}) = 0, \quad (4)$$

which is equivalent to finding an extremum of the gauge functional

$$F_U(g) = \frac{1}{4V} \sum_{x\mu} \frac{1}{2} \text{Tr} U_{x\mu}^g, \quad (5)$$

where $V = L^4$ is the lattice volume, with respect to gauge transformations g_x . After replacing $U \Rightarrow U^g$ at the extremum, the gauge condition (4) is satisfied. The manifold consisting of Gribov copies providing local maxima of the functional (5) and a semipositive Faddeev-Popov operator (see below) is called *Gribov region* Ω , while that of the global maxima is called the *fundamental modular domain* $\Lambda \subset \Omega$. Our gauge-fixing procedure is designed to approach this domain.

¹It is worthwhile to note that the DS approach, introduced originally as a method for resummation of the perturbative series, is not sensible for different gauge copies.

²Alternative algorithms to reach the fundamental modular region have been discussed in [31,32].

The gluon propagator D and its dressing function Z are then defined (for $p \neq 0$) by

$$D_{\mu\nu}^{ab}(p) = \frac{a^2}{g_0^2} \langle \tilde{A}_\mu^a(k) \tilde{A}_\nu^b(-k) \rangle = \left(\delta_{\mu\nu} - \frac{p_\mu p_\nu}{p^2} \right) \delta^{ab} D(p),$$

$$Z(p) = D(p) p^2, \quad (6)$$

where $\tilde{A}(k)$ represents the Fourier transform of the gauge potentials defined by Eq. (3) after having fixed the gauge, and a is the lattice spacing. The momentum p is given by $p_\mu = (2/a) \sin(\pi k_\mu/L)$, $k_\mu \in (-L/2, L/2]$. For $p \neq 0$, one gets, from Eq. (6),

$$D(p) = \frac{1}{9} \sum_{a=1}^3 \sum_{\mu=1}^4 D_{\mu\mu}^{aa}(p), \quad (7)$$

whereas at $p = 0$ the ‘‘zero-momentum propagator’’ $D(0)$ is defined as

$$D(0) = \frac{1}{12} \sum_{a=1}^3 \sum_{\mu=1}^4 D_{\mu\mu}^{aa}(p=0). \quad (8)$$

The lattice expression for the Landau-gauge Faddeev-Popov operator $M^{ab} = -\partial_\mu D_\mu^{ab}$ (where D_μ^{ab} denotes the covariant derivative in the adjoint representation) for $SU(2)$ is given by

$$M_{xy}^{ab}[U] = \sum_{\mu} \{ (\bar{S}_{x\mu}^{ab} + \bar{S}_{x-\hat{\mu};\mu}^{ab}) \delta_{x,y} - (\bar{S}_{x\mu}^{ab} - \bar{A}_{x\mu}^{ab}) \delta_{y,x+\hat{\mu}} - (\bar{S}_{x-\hat{\mu};\mu}^{ab} + \bar{A}_{x-\hat{\mu};\mu}^{ab}) \delta_{y,x-\hat{\mu}} \} \quad (9)$$

where

$$\bar{S}_{x\mu}^{ab} = \delta^{ab} \frac{1}{2} \text{Tr} U_{x\mu}, \quad \bar{A}_{x\mu}^{ab} = -\frac{1}{2} \epsilon^{abc} A_{x+\hat{\mu}/2;\mu}^c. \quad (10)$$

From the expression (10) it follows that a trivial zero eigenvalue is always present, such that at the Gribov horizon $\partial\Omega$ the first nontrivial zero eigenvalue appears. Thus, if the Landau gauge is properly implemented, $M[U]$ is a symmetric and semipositive matrix.

The ghost propagator $G^{ab}(x, y)$ is defined as [8,33]

$$G^{ab}(x, y) = \delta^{ab} G(x - y) \equiv \frac{1}{a^2} \langle (M^{-1})_{xy}^{ab}[U] \rangle. \quad (11)$$

Note that the ghost propagator becomes translational invariant (i.e., dependent only on $x - y$) and diagonal in color space only in the result of averaging over the ensemble of gauge-fixed representatives of the original Monte Carlo gauge configurations. The ghost propagator $G(p)$ in momentum space and its dressing function $J(p)$ can be written as

$$G(p) = \frac{a^2}{3V} \sum_{x,y,a} e^{-i(2\pi/L)k \cdot (x-y)} \langle (M^{-1})_{xy}^{aa}[U] \rangle, \quad (12)$$

$$J(p) = G(p) p^2,$$

where the coefficient $\frac{1}{3V}$ is taken for a full normalization,

including the indicated color average over $a = 1, 2, 3$. We mentioned above that $M[U]$ is symmetric and semipositive. In particular, it is positive-definite in the subspace orthogonal to constant vectors. The latter are zero modes of $M[U]$. Therefore, it can be inverted by using a conjugate-gradient method, provided that both the source $\psi^a(y)$ and the initial guess of the solution are orthogonal to zero modes. As a source, we adopted the one proposed in [4],

$$\psi^a(y) = \delta^{ac} e^{i(2\pi/L)k \cdot y}, \quad k \neq (0, 0, 0, 0), \quad (13)$$

for which the condition $\sum_y \psi^a(y) = 0$ is automatically imposed. Choosing the source in this way allows one to save computer time since, instead of the summation over x and y in Eq. (12), only the scalar product of $M^{-1} \psi$ with the source ψ itself has to be evaluated. In general, the gauge-fixed configurations can be used in a more efficient way if the inversion of M is done on sources for $c = 1, 2, 3$ such that the (adjoint) color averaging, formally required in Eq. (12), will be *explicitly* performed.

III. SIMULATION DETAILS

We restrict ourselves to Monte Carlo simulations at $\beta = 4/g_0^2 = 2.20$ and use lattice field configurations for which the gluon propagator has already been computed in [18]. Here we add the computation of the ghost propagator and new data obtained on the larger symmetric lattice with a linear size of $L = 40$. For the latter case we generated an ensemble of 430 independent Monte Carlo lattice field configurations. Consecutive configurations (considered as independent) were separated by 100 sweeps, each sweep comprised of one local heatbath update followed by $L/2$ microcanonical updates. In Table I we provide the full information for the field ensembles used throughout this paper.

For gauge fixing we employ the $Z(2)$ flip operation as discussed in [18]. This consists in flipping all link variables $U_{x\mu}$ attached and orthogonal to a 3d plane by multiplying them by -1 . Such global flips are equivalent to nonperiodic gauge transformations and represent an exact symmetry of the pure gauge action considered here. The Polyakov loops in the direction of the chosen links and averaged over

TABLE I. Lattice sizes, statistics, and number of gauge copies used throughout this paper. The second (third) column gives the number of configurations used to compute the gluon (ghost) propagators.

| L | Number of gl. prop. | Number of gh. prop. | N_{copy} |
|-----|---------------------|---------------------|-------------------|
| 8 | 200 | | 80 |
| 12 | 200 | | 80 |
| 16 | 240 | 60 | 24 |
| 24 | 346 | 157 | 24 |
| 32 | 247 | 118 | 40 |
| 40 | 430 | 64 | 80 |

the 3d plane obviously change their sign. Therefore, the flip operations combine, for each lattice field configuration, the 2^4 distinct gauge orbits (or Polyakov loop sectors) of strictly periodic gauge transformations into one larger gauge orbit. Let us note that the fundamental modular regions for the two procedures, i.e. with and without flips, might be different, at least for finite volume.

The second ingredient of our gauge-fixing procedure is the consequent use of the SA method, which has been found even computationally more efficient than the use of standard overrelaxation (OR).

The SA algorithm generates a field of gauge transformations $g(x)$ by Monte Carlo iterations with a statistical weight proportional to $\exp(4VF_U[g]/T)$. The “temperature” T is a technical parameter which is gradually decreased in order to maximize the gauge functional $F_U[g]$. In the beginning, T has to be chosen sufficiently large in order to allow traversing the configuration space of $g(x)$ fields in large steps. It has been checked that an initial value $T_{\text{init}} = 1.5$ is high enough. After each quasiequilibrium sweep, including both heatbath and microcanonical updates, T has been decreased with equal step size until $g(x)$ is uniquely captured in one basin of attraction. The criterion of success is that during the consecutively applied OR, the violation of transversality decreases in a more or less monotonous manner for almost all applications of the compound algorithm. This condition is reasonably satisfied for a final lower temperature value of $T_{\text{final}} = 0.01$ [34]. The number of temperature steps was chosen to be 1000 for the smaller lattice sizes and has been increased to 2000 for the lattice size 40^4 included here. The finalizing OR algorithm requires a number of iterations, varying from $O(10^2)$ to $O(10^3)$. In what follows we will call the combined algorithm employing SA (with finalizing OR) and $Z(2)$ flips the “FSA” algorithm.

Some details of the gauge-fixing procedure compared to our previous work [18] have been changed. For every configuration the Landau gauge was fixed $N_{\text{copy}} = 80$ times (5 gauge copies for every flip sector), each time starting from a random gauge transformation of the mother configuration, in this way obtaining N_{copy} Landau-gauge-fixed copies. In [18], where smaller lattices were simulated, N_{copy} was generally smaller. Only on very small lattices (12^4 and 8^4), where producing copies was substantially cheaper, did we also produce 80 copies.

In order to reduce the computational effort in the finalizing OR sweeps on the 40^4 lattice, we applied the following trick. We noticed that after a comparably small number of OR sweeps, definitely before the convergence criterion is reached, one can already decide which copy has a higher maximum of the gauge functional; i.e. one can stop the OR procedure when the change in the functional becomes comparably small and further sweeps will not change the order of copies according to the value of the maximized functional. Note that the functional differed from its final

value only in the eighth digit, and we used these values below in Fig. 7. After having selected the “best copy” (bc), the OR gauge fixing for this copy has to be finalized. To be precise, the randomly chosen “first copy” (fc) was also completely gauge fixed, just for the purpose of comparison.

For the finalizing OR we used the standard Los Alamos-type overrelaxation with the parameter $\omega = 1.7$. For the bc and the fc, the iterations are stopped when the following transversality condition is satisfied:

$$\max_{x,a} \left| \sum_{\mu=1}^4 (A_{x+\hat{\mu}/2;\mu}^a - A_{x-\hat{\mu}/2;\mu}^a) \right| < \epsilon_{\text{lor}}. \quad (14)$$

We used the value $\epsilon_{\text{lor}} = 10^{-7}$ [i.e. 10^{-14} for $(\partial A)^2$].

IV. RESULTS

In this section we present the data for the gluon and ghost propagators. In Fig. 1 we show the new data for the gluon propagator $D(p)$ in physical units, obtained on the 40^4 lattice at $\beta = 2.20$. We compare the bc FSA result with the fc SA result (the latter without flips). We clearly see the Gribov copy effect for the lowest accessible momenta moving the data points to lower values for better copies (with the larger gauge functional). The different points at $p \sim 300$ MeV belong to different realizations of p^2 and seem to indicate some violation of the hypercubic symmetry.

In Fig. 2 we present these new data together with the ones obtained on smaller lattice sizes, always for the bc FSA case.

We see that the data are nicely consistent with each other and indicate a turnover to decreasing values towards vanishing momenta. A smooth extrapolation to $D(0)$ becomes visible. But still, there is no indication for a vanishing gluon propagator at zero momentum for increasing vol-

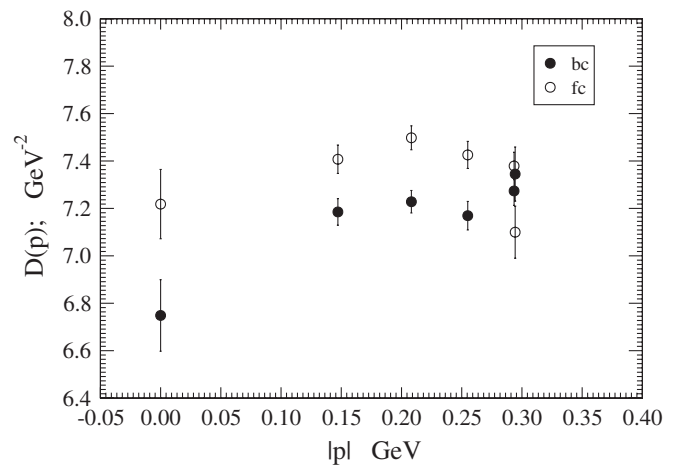


FIG. 1. The momentum dependence and Gribov copy sensitivity of the gluon propagator $D(p)$ in the IR region on the 40^4 lattice. Filled symbols correspond to the bc FSA ensemble, open symbols to the fc SA ensemble.

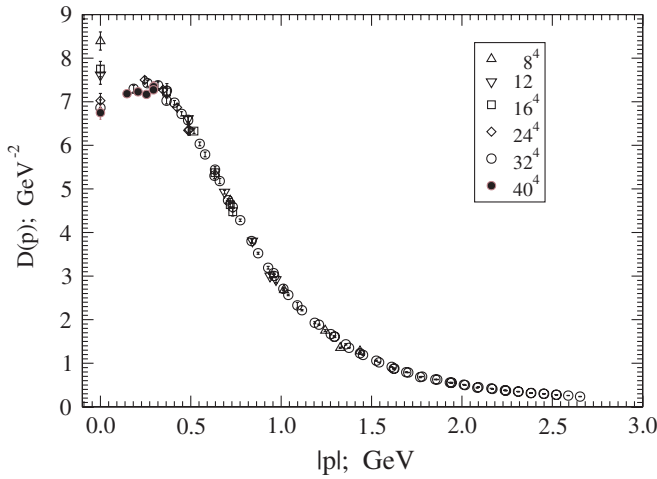


FIG. 2 (color online). The momentum dependence of the gluon propagator $D(p)$ on various lattice sizes. The bc results are shown throughout.

ume. This is demonstrated in Fig. 3, where we show the dependence of the zero-momentum propagator $D(0)$ as a function of the inverse linear lattice size $1/L$. This behavior demonstrates a (slight) tendency to decrease, and hardly seems consistent with the $D(0) = 0$ limit. Rather, one could consider it as an argument in favor of the *decoupling* solution, with a finite gluon propagator in the infrared. However, one still cannot exclude that there are even more efficient gauge-fixing methods, superior to the one we use, which could make this decrease more drastic.

Using Ward-Slavnov-Taylor identities the authors of [25,27,35] came to the conclusion that the gluon propagator should be IR divergent; however, this divergence might be so weak that it could hardly be resolved on the lattice. We believe that our results for $D(0)$ are in clear disagreement with even a weak divergence.

Analogously to Fig. 1, in Fig. 4 we show the ghost dressing function $J(p)$ obtained on the 40^4 lattice. There

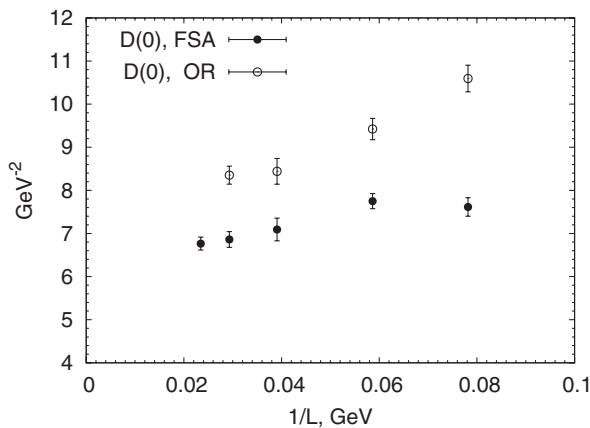


FIG. 3. The dependence of $D(0)$ on the lattice size. The bc FSA results are compared with the fc OR results (without flips).

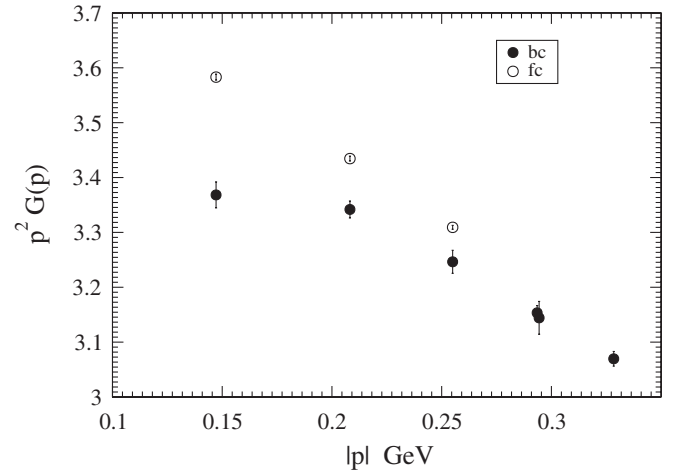


FIG. 4. The momentum dependence and Gribov copy sensitivity of the ghost dressing function $J(p) = p^2 \cdot G(p)$ in the IR region on the 40^4 lattice. Filled symbols correspond to the bc FSA ensemble, open symbols to the fc SA ensemble.

is a very clear Gribov copy effect changing $J(p)$ even qualitatively. Whereas the fc SA results seem to support a weakly singular behavior, the bc FSA data provide a *plateau* pointing to a finite IR value of the ghost dressing function, i.e. a tree-level behavior of the ghost propagator. Our data indicate that the plateau starts at $p \lesssim 200$ MeV.

In Fig. 5 the ghost dressing function is shown for lattice sizes from 16^4 to 40^4 . We always show bc FSA results, except for 24^4 , where we also compare with fc data obtained with the conventional OR algorithm. The latter show an even stronger IR singular behavior than those data obtained with the fc SA algorithm.

Thus, increasing the lattice size up to 40^4 and applying the FSA procedure, we observe a deviation from the weak singular behavior towards a plateau consistent with the

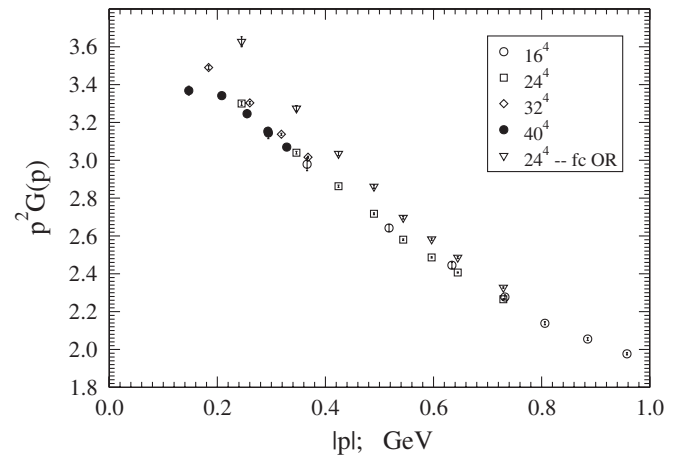


FIG. 5. The momentum dependence of the ghost dressing function $p^2 \cdot G(p)$ on the various lattices. For comparison, results obtained with the OR algorithm on 24^2 lattices are also shown.

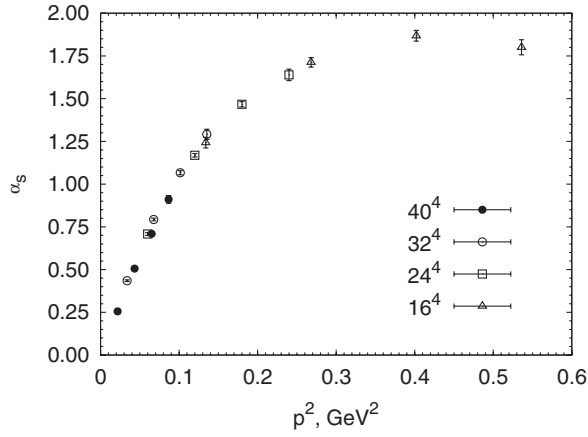


FIG. 6. The momentum dependence of the running coupling in the infrared region.

decoupling solutions and in contradiction with the Kugo-Ojima confinement criterion.

In Fig. 6, for the bc FSA results obtained on lattice sizes from 16^4 up to 40^4 , we show the behavior of the running coupling related to the ghost-ghost-gluon vertex,

$$\alpha_s(p) = \frac{g_0^2}{4\pi} J^2(p) Z(p), \quad (15)$$

under the assumption that the vertex function is constant, as seen in perturbation theory [36] and also approximately in lattice simulations [37,38].

The decrease towards $p^2 = 0$ is obvious. With the improved gauge fixing the effect is even strengthened, such that an approach to an IR fixed point, as expected from the scaling DS and FRG solutions, seems to be excluded.

V. DISCUSSION: THE QUALITY OF THE GAUGE-FIXING PROCEDURE

In most of our simulations we have generated up to $N_{\text{copy}} = 80$ for every thermalized configuration (up to 5 gauge copies for every flip sector). A very reasonable question is whether our results will change if we further increase the number of gauge copies, N_{copy} . In Fig. 7 we show the dependence of the average bc functional $\langle F_{\text{bc}} \rangle \times (k_{\text{copy}})$:

$$\langle F_{\text{bc}} \rangle(k_{\text{copy}}) = \frac{1}{n} \sum^n F_{\text{bc}}(k_{\text{copy}}), \quad k_{\text{copy}} = 1, \dots, N_{\text{copy}}, \quad (16)$$

where for every configuration $F_{\text{bc}}(k_{\text{copy}})$ is the “best” (i.e., maximal) value of the functional F found after employing k_{copy} copies, and n denotes the number of configurations.

One can see that this average still has a tendency to grow, which could mean that one would need even more copies to reach the global maxima. To understand it better, we generated 25 configurations on the 40^4 lattice with $N_{\text{copy}} = 320$ (i.e., 20 gauge copies per sector).

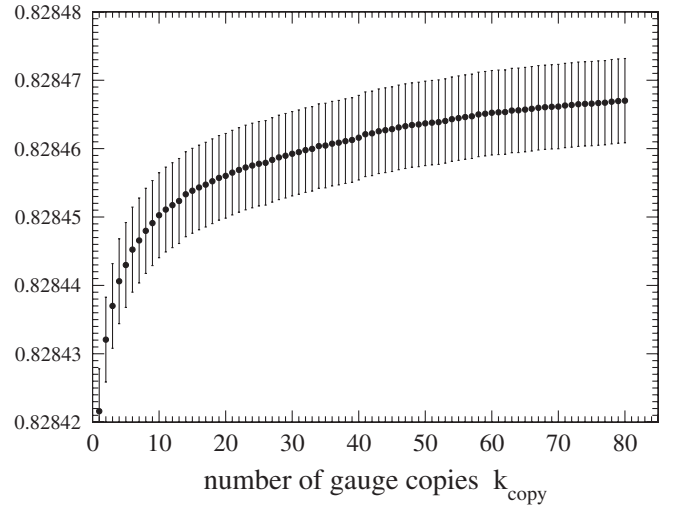


FIG. 7. The average value of the *best* gauge functional $\langle F_{\text{bc}} \rangle \times (k_{\text{copy}})$ as a function of the number of selected gauge copies k_{copy} for a 40^4 lattice.

In Fig. 8 we show the difference

$$\Delta F(k_{\text{copy}}) = F_{\text{bc}}(k_{\text{copy}}) - F_{\text{bc}}(80) \quad (17)$$

at $k_{\text{copy}} = 160, 240,$ and 320 for these configurations.

For the majority of configurations this difference is rather small. However, for about 20% of configurations the difference is of the order of 10^{-5} , which could still mean a rather strong influence on the values of the propagators.

To demonstrate that the change in the functional of the order of 10^{-5} indeed might give rise to a substantial change in the propagators, we plot in Fig. 9 the gluon propagator computed on a 32^4 lattice at two momenta, $p = 0$ and $p = p_{\text{min}}$, as a function of the difference $F_{\text{bc}}(32) - F_{\text{bc}}(k_{\text{copy}})$ for $k_{\text{copy}} = 1, 2, \dots, 18$. One can see that the change in the

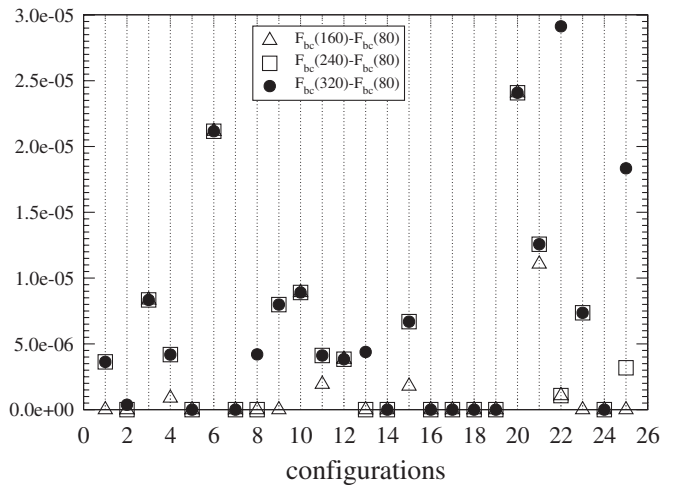


FIG. 8. The difference $F_{\text{bc}}(k_{\text{copy}}) - F_{\text{bc}}(k_{\text{copy}} = 80)$ for various numbers of the gauge copies k_{copy} for a 40^4 lattice.

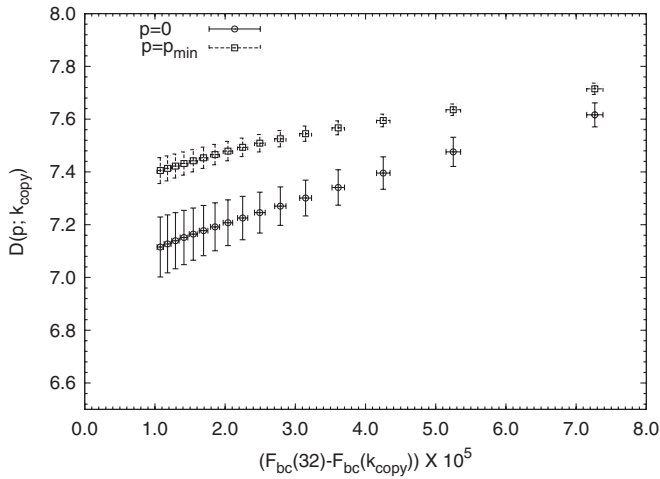


FIG. 9. The gluon propagator at momenta $p = 0$ and $p = p_{min}$ vs the functional F_{bc} for a 32^4 lattice.

functional F_{bc} in the fifth digit brings quite a substantial change in the propagator at both momenta.

These observations show that there might be *another* even more efficient gauge-fixing method which will be more successful in the search of the global maximum of the functional F (as FSA is superior with respect to standard OR).

Therefore, we cannot draw a final conclusion before spending much more effort on the optimization of the gauge-fixing procedure. However, we expect that both the gluon propagator and the ghost propagator will take even lower values in the infrared, when approaching the fundamental modular region.

VI. CONCLUSIONS

In this work we studied numerically the dependence of the Landau-gauge gluon and ghost propagators, as well as of the running coupling constant, in pure gauge $SU(2)$ lattice theory in the infrared region. Special emphasis has been made on the study of the dependence of these “observables” on the choice of Gribov copies.

The simulations have been performed using the standard Wilson action at $\beta = 2.20$ for linear lattice sizes up to $L = 40$. For gauge fixing, gauge orbits enlarged by $Z(2)$ flip operations were considered with up to 5 gauge copies in every flip sector (in total, up to 80 gauge copies). For 25 thermalized configurations we produced 20 copies per sector (in total, 320 gauge copies for every configuration). The maximization of the gauge functional was achieved by the simulated annealing method which was always combined with consecutive overrelaxation (“FSA” algorithm).

Our findings can be summarized as follows.

- (1) For the gluon propagator our new data for the 40^4 lattice agree with data on the smaller lattices (up to 32^4). We confirm our conclusion [18] about the appearance of the maximum at a nonzero value of

the momentum p^2 (this maximum was absent for lattice sizes $\leq 24^4$).

The zero-momentum gluon propagator $D(0)$ has a tendency to decrease with growing lattice size L . This observation is in clear contradiction with the infrared divergent gluon propagator obtained on the basis of Ward-Slavnov-Taylor identities.

For the time being, this behavior hardly seems consistent with a $D(0) = 0$ limit at infinite L , and could be considered rather like an argument in favor of the *decoupling* solution with a nonsingular gluon propagator. However, we do not yet consider the problem of the infrared asymptotics of the gluon propagator resolved (see below).

- (2) We calculated the ghost propagator for lattices up to 40^4 . Our bc dressing function $J(p)$ of the ghost propagator demonstrates the approach to a *plateau* in the infrared, while the fc dressing function still grows (as in earlier calculations; see, e.g., [3,29,39]).

This is a clear indication of the lack of IR enhancement of the ghost propagator. This plateau behavior is in clear contradiction with the Kugo-Ojima confinement criterion. The fate of this confinement criterion still needs further clarification.

- (3) We have found that the effect of Gribov copies is essential in the infrared range $p < 1$ GeV for both propagators and as a consequence for the running coupling. Therefore, the *quality* of the gauge-fixing procedure in the study of gauge dependent observables remains important.

Indeed, the FSA method provides systematically higher values of the functional $F_U(g)$ as compared to the standard OR procedure for the same thermalized configurations. This means that, in practice, OR needs many more random copies to explore (correspondingly, much more CPU time to spend) to find larger values of $F_U(g)$ as compared to FSA. This effect becomes stronger with increasing volume. However, we cannot say that we have reached the fundamental modular region when fixing the Landau gauge on larger lattices. One cannot exclude other methods that may be superior to our FSA algorithm. We believe that the Gribov problem deserves even more thorough study.

Perhaps there are alternative ways to resolve the problem of the IR asymptotics of the propagators. We have to be aware that the lattice method, as it is normally used, still has some uncertainties. First of all, the continuum limit in the infrared range is hard to control and it depends on the proper choice of the gauge potential $\mathcal{A}_{x\mu}$. Moreover, the infrared limit is sensitive to the boundary conditions, which normally are taken to be periodic. Incomplete gauge fixing, in combination with these choices, seems to unavoidably lead to zero-momentum modes that are not sufficiently suppressed even in the thermodynamic limit. That the presence of zero-momentum modes can spoil the

behavior of gauge-variant propagators is well known from the example of 4d compact $U(1)$ lattice gauge theory [40–42]. Whether a BRST conformal lattice reformulation will solve the issue, as proposed in [43,44], remains to be seen.

ACKNOWLEDGMENTS

This investigation has been partly supported by the Heisenberg-Landau program of collaboration between the Bogoliubov Laboratory of Theoretical Physics of the Joint Institute for Nuclear Research Dubna (Russia) and

German institutes, and partly by the joint DFG-RFBR Grant No. 436 RUS 113/866/0-1 and the RFBR-DFG Grant No. 06-02-04014. V. B. and V. M. are supported by the Grant for Scientific Schools, No. NSh-679.2008.2. V. B. is supported by Grant No. RFBR 07-02-00237-a and No. RFBR 08-02-00661-a. M. M. P. gratefully acknowledges useful discussions with E.-M. Ilgenfritz, A. Maas, J. Pawłowski, C. Fischer, O. Pene, L. von Smekal, and A. Sternbeck.

-
- [1] J.E. Mandula and M. Ogilvie, *Phys. Lett. B* **185**, 127 (1987).
 - [2] L. Giusti, M.L. Paciello, C. Parrinello, S. Petrarca, and B. Taglienti, *Int. J. Mod. Phys. A* **16**, 3487 (2001).
 - [3] A. Cucchieri and T. Mendes, *Proc. Sci., LAT2007* (2007) 297.
 - [4] A. Cucchieri, *Nucl. Phys.* **B508**, 353 (1997).
 - [5] T.D. Bakeev, E.-M. Ilgenfritz, V.K. Mitrjushkin, and M. Müller-Preussker, *Phys. Rev. D* **69**, 074507 (2004).
 - [6] I.L. Bogolubsky, G. Burgio, V.K. Mitrjushkin, and M. Müller-Preussker, *Phys. Rev. D* **74**, 034503 (2006).
 - [7] V.N. Gribov, *Nucl. Phys.* **B139**, 1 (1978).
 - [8] D. Zwanziger, *Nucl. Phys.* **B412**, 657 (1994).
 - [9] I. Ojima, *Nucl. Phys.* **B143**, 340 (1978).
 - [10] T. Kugo and I. Ojima, *Prog. Theor. Phys. Suppl.* **66**, 1 (1979).
 - [11] R. Alkofer and L. von Smekal, *Phys. Rep.* **353**, 281 (2001).
 - [12] C. Wetterich, *Phys. Lett. B* **301**, 90 (1993).
 - [13] J.M. Pawłowski, D.F. Litim, S. Nedelko, and L. von Smekal, *Phys. Rev. Lett.* **93**, 152002 (2004).
 - [14] D. Zwanziger, *Phys. Rev. D* **65**, 094039 (2002).
 - [15] D. Zwanziger, *Phys. Rev. D* **67**, 105001 (2003).
 - [16] D. Dudal, R.F. Sobreiro, S.P. Sorella, and H. Verschelde, *Phys. Rev. D* **72**, 014016 (2005).
 - [17] D. Dudal, S.P. Sorella, N. Vandersickel, and H. Verschelde, *Phys. Rev. D* **77**, 071501 (2008).
 - [18] I.L. Bogolubsky, V.G. Borniyakov, G. Burgio, E.-M. Ilgenfritz, V.K. Mitrjushkin, and M. Müller-Preussker, *Phys. Rev. D* **77**, 014504 (2008).
 - [19] C.S. Fischer, A. Maas, and J.M. Pawłowski, arXiv:0810.1987.
 - [20] L. von Smekal, R. Alkofer, and A. Hauck, *Phys. Rev. Lett.* **79**, 3591 (1997).
 - [21] L. von Smekal, A. Hauck, and R. Alkofer, *Ann. Phys. (N.Y.)* **267**, 1 (1998).
 - [22] C. Lerche and L. von Smekal, *Phys. Rev. D* **65**, 125006 (2002).
 - [23] C.S. Fischer and J.M. Pawłowski, *Phys. Rev. D* **75**, 025012 (2007).
 - [24] D. Zwanziger, *Nucl. Phys.* **B364**, 127 (1991).
 - [25] P. Boucaud *et al.*, *Eur. Phys. J. A* **31**, 750 (2007).
 - [26] A.C. Aguilar, D. Binosi, and J. Papavassiliou, *Phys. Rev. D* **78**, 025010 (2008).
 - [27] P. Boucaud *et al.*, *J. High Energy Phys.* 06 (2008) 099.
 - [28] A. Cucchieri and T. Mendes, *Phys. Rev. Lett.* **100**, 241601 (2008).
 - [29] I.L. Bogolubsky, E.-M. Ilgenfritz, M. Müller-Preussker, and A. Sternbeck, *Proc. Sci., LAT2007* (2007) 290.
 - [30] D. Dudal, J.A. Gracey, S.P. Sorella, N. Vandersickel, and H. Verschelde, *Phys. Rev. D* **78**, 065047 (2008).
 - [31] O. Oliveira and P.J. Silva, *Comput. Phys. Commun.* **158**, 73 (2004).
 - [32] A. Maas, *Phys. Rev. D* **79**, 014505 (2009).
 - [33] H. Suman and K. Schilling, *Phys. Lett. B* **373**, 314 (1996).
 - [34] P. Schemel, Diploma thesis, Humboldt University Berlin/Germany, 2006.
 - [35] P. Boucaud *et al.*, *J. High Energy Phys.* 03 (2007) 076.
 - [36] J.C. Taylor, *Nucl. Phys.* **B33**, 436 (1971).
 - [37] A. Cucchieri, T. Mendes, and A. Mihara, *J. High Energy Phys.* 12 (2004) 012.
 - [38] E.-M. Ilgenfritz, M. Müller-Preussker, A. Sternbeck, A. Schiller, and I.L. Bogolubsky, *Braz. J. Phys.* **37**, 193 (2007).
 - [39] A. Cucchieri and T. Mendes, *Phys. Rev. D* **78**, 094503 (2008).
 - [40] V.K. Mitrjushkin, *Phys. Lett. B* **389**, 713 (1996).
 - [41] I.L. Bogolubsky, V.K. Mitrjushkin, M. Müller-Preussker, and P. Peter, *Phys. Lett. B* **458**, 102 (1999).
 - [42] I.L. Bogolubsky, V.K. Mitrjushkin, M. Müller-Preussker, P. Peter, and N.V. Zverev, *Phys. Lett. B* **476**, 448 (2000).
 - [43] L. von Smekal, D. Mehta, A. Sternbeck, and A.G. Williams, *Proc. Sci., LAT2007* (2007) 382.
 - [44] L. von Smekal, M. Ghiotti, and A.G. Williams, *Phys. Rev. D* **78**, 085016 (2008).